SURFACE MICROSCOPY

Visualizing H_2O molecules reacting at TiO_2 active sites with transmission electron microscopy

Wentao Yuan[1]*, Beien Zhu[2,3]*, Xiao-Yan Li[2,4]*, Thomas W. Hansen[5], Yang Ou[1], Ke Fang[1], Hangsheng Yang[1], Ze Zhang[1]†, Jakob B. Wagner[5]†, Yi Gao[2,3]†, Yong Wang[1]†

Imaging a reaction taking place at the molecular level could provide direct information for understanding the catalytic reaction mechanism. We used in situ environmental transmission electron microscopy and a nanocrystalline anatase titanium dioxide (001) surface with (1 × 4) reconstruction as a catalyst, which provided highly ordered four-coordinated titanium "active rows" to realize real-time monitoring of water molecules dissociating and reacting on the catalyst surface. The twin-protrusion configuration of adsorbed water was observed. During the water–gas shift reaction, dynamic changes in these structures were visualized on these active rows at the molecular level.

Imaging at the atomic scale with transmission electron microscopy (TEM) has benefited from the developments of aberration correctors and in situ equipment (*1*–*8*). For studies of heterogeneous catalysts, these developments, along with approaches that allow gases and even liquids to contact samples [known as environmental TEM (ETEM)], have enabled imaging of single molecules and atoms adsorbed on a catalyst surface (*9*–*14*). However, the direct visualization of gas molecules reacting at catalytic sites is generally difficult to achieve with TEM. Normally, the molecules that adsorb and react dynamically do not offer sufficient contrast for TEM identification. We now show that this obstacle can be overcome by taking advantage of the highly ordered four-coordinated Ti (Ti_{4c}) rows (termed "active rows," owing to their lower coordination) on the anatase TiO_2 (1×4)-(001) surface [i.e., a TiO_2(001) surface with (1 × 4) reconstruction] to facilitate enhanced contrast of adsorbing molecules along the row direction and allow real-time monitoring of H_2O species dissociating and reacting on the catalyst surface.

The atomic structure of the TiO_2 (1×4)-(001) surface has been characterized by both aberration-corrected ETEM and scanning transmission electron microscopy (STEM) images. The bulk-truncated (1×1)-(001) surface usually reconstructs to a (1×4)-(001) surface (Fig. 1, A to C) by periodically replacing the surface oxygen rows (along the [010] direction) with TiO_3 ridges every four unit cells along the TiO_2[100] direction (*15*–*17*). As a result, protruded Ti_{4c} rows are periodically exposed on the surface and show distinct contrast, so the subtle changes occurring in reactions could be detected by means of ETEM observation without contrast overlap. The ordered Ti_{4c} active rows could provide sufficient contrast for direct ETEM visualization of water if the molecules adsorbed in ordered arrays.

We synthesized TiO_2 nanocrystals with exposed {001} facets by a hydrothermal route (see supplementary materials) (*18*, *19*). The nanocrystals were heated in oxygen in situ (~10^{-3} mbar) at 500° to 700°C to trigger the reconstruction. The reconstructed structures remained stable in this temperature range, in accord with recent ETEM studies (*15*, *16*, *20*). During the ETEM experiments, we used a constant electron beam dose with a small value (<1 A/cm^2), and no appreciable irradiation damage was observed on the TiO_2 surface (*21*). After heating at 700°C for ~10 min, the reconstructed TiO_2 (1×4)-(001) surface of an admolecule (ADM) configuration was obtained, as confirmed by the ETEM image (Fig. 1D), in which the protruding black dots represent the Ti_{4c} rows. The ADM structure did not change appreciably after ~16 min of intermittent TEM observation.

[1]State Key Laboratory of Silicon Materials and Center of Electron Microscopy, School of Materials Science and Engineering, Zhejiang University, Hangzhou, 310027 China. [2]Division of Interfacial Water and Key Laboratory of Interfacial Physics and Technology, Shanghai Institute of Applied Physics, Chinese Academy of Sciences, Shanghai, 201800 China. [3]Shanghai Advanced Research Institute, Chinese Academy of Sciences, Shanghai, 201210 China. [4]University of Chinese Academy of Sciences, Beijing, 100049 China. [5]DTU Nanolab, Technical University of Denmark, DK-2800, Kgs. Lyngby, Denmark.
*These authors contributed equally to this work.
†Corresponding author. Email: yongwang@zju.edu.cn (Y.W.); gaoyi@zjlab.org.cn (Y.G.); jakob.wagner@cen.dtu.dk (J.B.W.); zezhang@zju.edu.cn (Z.Z.)

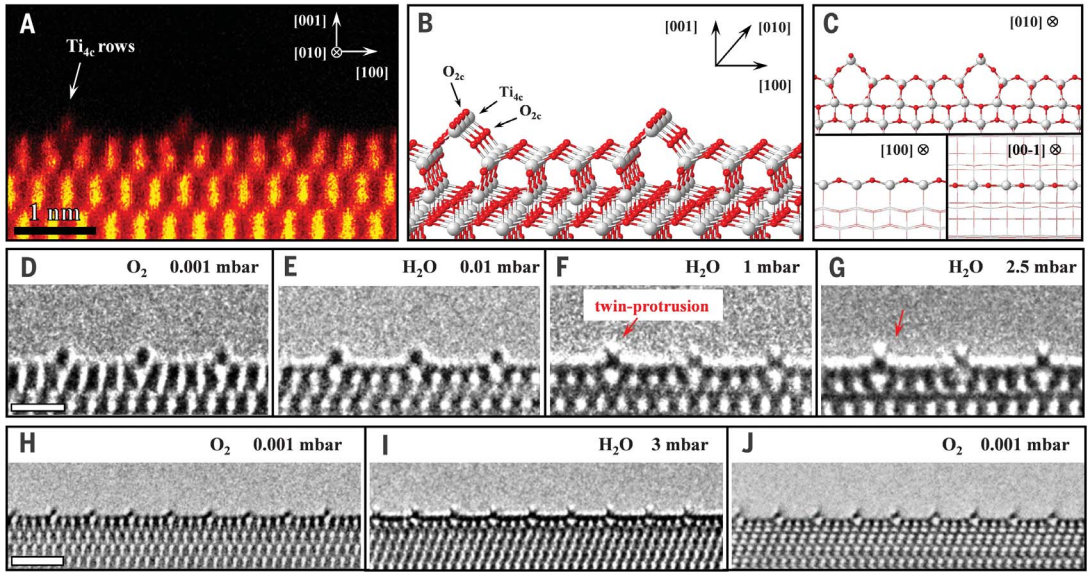

Fig. 1. Dynamic atomic structural evolution of the (1×4) reconstructed TiO_2(001) surface in a water vapor environment. (**A**) High-angle annual dark-field–STEM image of the (1×4)-(001) surface, viewed from the [010] direction. The image was acquired at 700°C in vacuum (TEM column pressure: ~10^{-7} mbar). (**B**) ADM reconstruction models of the (1×4)-(001) surface (Ti, gray; O, red). (**C**) Atomic models of a Ti_{4c} row. (**D** to **G**) Aberration-corrected in situ ETEM images show the same area of TiO_2(001) surface at 700°C under oxygen [(D), 0.001 mbar] and water vapor [(E), 0.01 mbar; (F), 1 mbar; (G), 2.5 mbar] conditions. Scale bar, 1 nm. (**H** to **J**) Another case shows the reversible structural transition induced by a change in the gas environment at 700°C from oxygen [(H), 0.001 mbar] to water vapor [(I), 3 mbar] and then reversion to oxygen [(J), 0.001 mbar]. Scale bar, 2 nm.

The O_2 gas was then evacuated, and H_2O vapor (fig. S1) was introduced at the same temperature. When the H_2O pressure was raised to 1 mbar, two additional small protrusions were observed at the top of the Ti_{4c} rows (Fig. 1F). This twin-protrusion structure became more resolved for a H_2O pressure of 2.5 mbar, owing to a higher water surface coverage (Fig. 1G and movie S1). At both pressures, the twin-protrusion structure remained visible during the TEM observation. When the background environment was changed from H_2O to O_2 or vacuum, the twin-protrusion structure disappeared (Fig. 1, H and J, and fig. S2). The electron beam was switched off after acquisition of the image in Fig. 1H and then H_2O was introduced; a snapshot (Fig. 1I) obtained ~5 min later still shows the twin-protrusion structure, which excludes the effect of the electron beam in its formation. We also ruled out the defocus effect of TEM imaging in different gas environments (figs. S3 to S5). Because the TiO_2 surface did not undergo any other structural changes, we attributed the twin protrusions to an adsorbed water species.

We performed in situ Fourier transform infrared spectroscopy (FTIR) to characterize the surface adsorption species. We heated the TiO_2 crystals to 500°C in vacuum to obtain the (1×4)-(001) surface. Under these conditions, no obvious valley was observed in the hydroxyl region (blue trace in Fig. 2A). Water vapor (5 mbar) was introduced into the in situ FTIR reactor to mimic the in situ TEM experimental condition. About 20 min later, we started to acquire the spectrum and observed two valleys in the hydroxyl region at 3717 and 3663 cm^{-1}. We assigned both features to the adsorbed species on the Ti_{4c} rows (*22*, *23*), because previous studies have shown that the water molecules only chemically adsorb at the Ti_{4c} ridges on the (1×4)-(001) surface (*24*). This indicates that the twin-protrusion structure observed in the ETEM experiments (also at 500°C; see fig. S6) was composed of two different hydroxyl species.

We used density functional theory (DFT) to examine the different adsorbed water structures on the (1×4)-(001) surface (figs. S7 and S8 and appendix S1). At low coverage, one dissociative H_2O adsorbs stably at the Ti_{4c} site by transforming the H atom to the adjacent O_{2c} atom and cleaving the Ti_{4c}–O_{2c} bond. With increasing coverage, the stability of the dissociatively adsorbed H_2O structure decreases because of the increased stress in the reconstructed substrate, in agreement with recently reported results (*25*). Instead, the relative stability of the structure with two symmetric protrusions (each is an OH–H_2O group) (Fig. 2, B to D) increases because it does not induce additional stress at higher coverages (fig. S9). The structure has comparable adsorption energy per H_2O molecule with the dissociatively adsorbed H_2O at ½ coverage. The stability of this twin-protrusion structure becomes compelling when the coverage reaches 1, corresponding to the experimental condition as calculated by combining the adsorption energy with the thermodynamic adsorption isotherm (*26*, *27*). On the basis of this atomic structure, a simulated high-resolution TEM image (fig. S10B) was generated, in agreement with the ETEM image (fig. S10A). In addition, the calculated vibration frequencies of the twin protrusions at 3695 and 3652 cm^{-1}, respectively, were consistent with the in situ FTIR results.

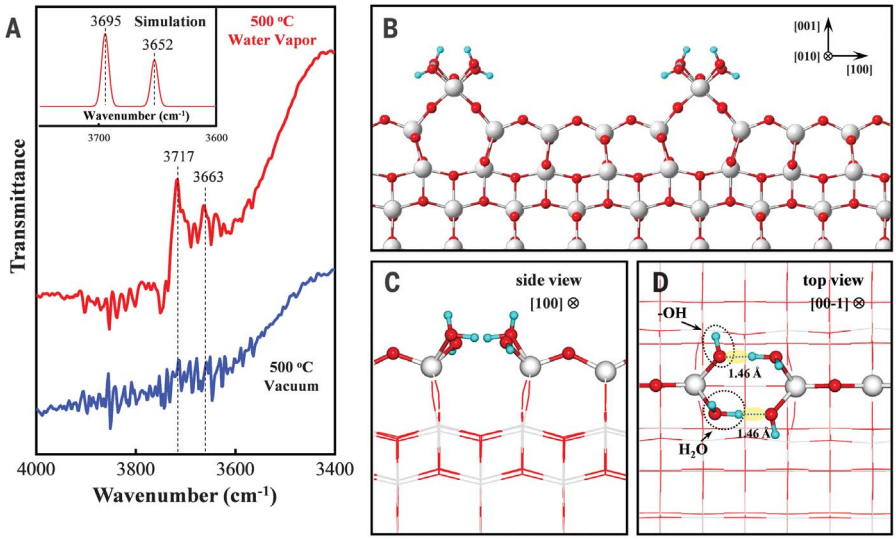

Fig. 2. The twin-protrusion configuration of adsorbed water. (**A**) In situ FTIR spectra of the hydroxyl region for TiO_2 in the presence of water vapor (5 mbar; 500°C) and vacuum (10^{-6} mbar; 500°C). The inset shows results of a theoretical simulation. (**B** to **D**) Atomic structure of the adsorbed H_2O species on the TiO_3 rows, as verified by theoretical calculations, viewed from the [010] direction (B), the [100] direction (C), and the [00-1] direction (D) (gray, Ti; red, O; cyan, H).

Because TiO_2 can catalyze the water–gas shift reaction ($H_2O + CO \rightarrow H_2 + CO_2$) at elevated temperatures (*28*, *29*), we studied this reaction by introducing CO into the ETEM column. The gas environment was changed from pure water vapor (2.5 mbar) to a mixed gas environment (CO and H_2O vapor in a 1:1 ratio; pressure: 5 mbar). Under these conditions, the twin-protrusion structure became unstable (Fig. 3A and movie S2). Its contrast changed dynamically: Most of the time it was blurred, but it would occasionally clear (Fig. 3B), with no substantial contrast change observed in TiO_2 bulk and in other surface areas. For example, in one case the twin protrusion was clearly seen initially [Fig. 3B, (1)], almost disappeared after 2.2 s [Fig. 3B, (2)], and then reappeared at 4 s [Fig. 3B, (3)]. The disappearance and reappearance occurred again at 5.8 s [Fig. 3B, (4)] and 7.8 s [Fig. 3B, (5)], respectively. The contrast change of the twin protrusions was also evidenced by the intensity profiles across the protruding row (Fig. 3C). Similar cases are shown in fig. S11 and movie S3. In a pure water vapor environment, the twin protrusions did not display such contrast changes (fig. S12 and movie S1), hence ruling out electron beam effects for the disappearances and reappearances.

Thus, the dynamic change of twin protrusions in mixed gas environments suggests that the adsorbed hydroxyls were reacting with CO molecules, which indicates that the Ti_{4c} sites are the reaction sites. In addition, because the net free-energy change of this reaction is negative (–3.76 kJ mol^{-1} under the experimental condition) and the known conversion temperatures are generally lower than 700°C (*28*, *29*), it is reasonable to conclude that the observed reaction was not induced by the electron beam. The reaction pathway of the twin-protrusion–adsorbed H_2O species with CO molecules was calculated by DFT (fig. S13). During the reaction, the H_2O species of the twin protrusion are consumed by CO gas and supplemented by H_2O vapor repeatedly, which relates to the dynamic contrast change observed experimentally. In the reaction cycle (fig. S13), the two largest energy barriers come from H_2O dissociation of the twin-protrusion (0.48 eV) and single OH–H_2O (0.57 eV) structures, which indicates that these are two relatively stable structures with comparatively long lifetimes. Thus, a changing mixture of single OH–H_2O and twin-protrusion structures was imaged by TEM. The contrast of the twin protrusions would occasionally clear when they were the majority on one of the active rows [Fig. 3B, (2) and (4)].

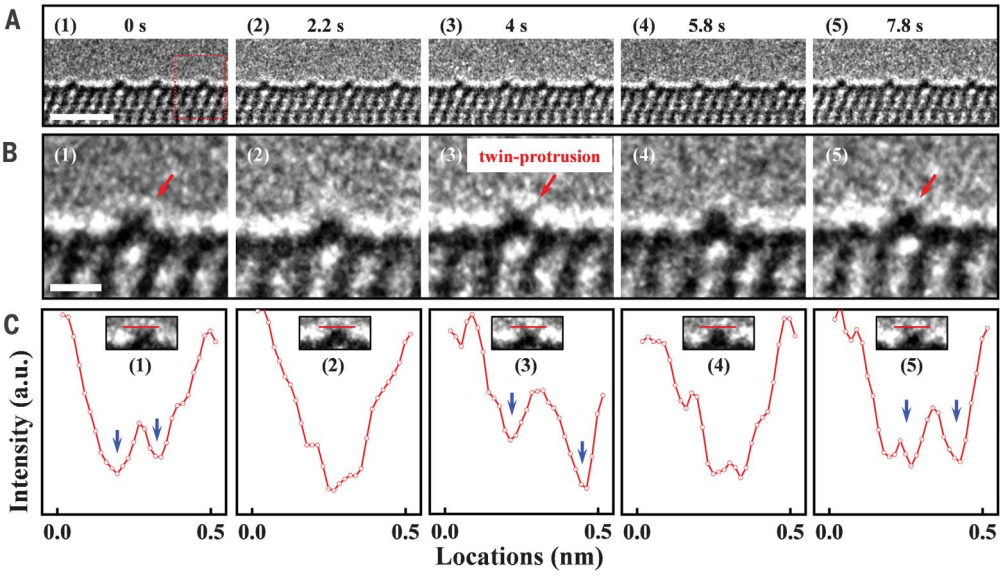

Fig. 3. Dynamic structural evolution of the (1 × 4)-(001) surface in the water–gas shift reaction. (**A**) Sequential ETEM images acquired in the mixed gas environment (1:1 ratio of CO and H_2O vapor; gas pressure: 5 mbar; temperature: 700°C), viewed from the [010] direction. Scale bar, 2 nm. (**B**) Enlarged ETEM images show the dynamic structural evolution of the Ti row outlined by the dotted rectangle in (A). Scale bar, 0.5 nm. (**C**) Intensity profiles along the lines crossed the Ti rows of (B). Blue arrows denote intensity valleys corresponding to the twin protrusions. a.u., arbitrary units.

Most of the time, the contrast is blurred because of the interference between the two structures [Fig. 3B, (1), (3), and (5)]. The single OH–H_2O structure was not obviously visualized via TEM, as shown by the simulated image (fig. S14).

By visualizing and monitoring the adsorbed water species on the ridge of the (1×4)-(001) TiO_2 surface, we confirmed that the Ti_{4c} atoms on the ridge are active sites for H_2O dissociation and reaction. The direct TEM visualization revealed an adsorbed water structure with a twin-protrusion feature on the TiO_2 surface. This work demonstrates that in situ ETEM can be used to monitor a catalytic process taking place at highly ordered active sites.

REFERENCES AND NOTES

1. D. A. Muller, *Nat. Mater.* **8**, 263–270 (2009).
2. D. S. Su, B. Zhang, R. Schlögl, *Chem. Rev.* **115**, 2818–2882 (2015).
3. L. DeRita *et al.*, *Nat. Mater.* **18**, 746–751 (2019).
4. L. Luo *et al.*, *Nat. Mater.* **17**, 514–518 (2018).
5. L. Zou *et al.*, *Nat. Mater.* **17**, 56–63 (2018).
6. L. Zhang, B. K. Miller, P. A. Crozier, *Nano Lett.* **13**, 679–684 (2013).
7. K. Sytwu *et al.*, *Nano Lett.* **18**, 5357–5363 (2018).
8. Y. Lin *et al.*, *Phys. Rev. Lett.* **111**, 156101 (2013).
9. C. L. Jia, M. Lentzen, K. Urban, *Science* **299**, 870–873 (2003).
10. M. Koshino *et al.*, *Science* **316**, 853 (2007).
11. Z. Liu, K. Yanagi, K. Suenaga, H. Kataura, S. Iijima, *Nat. Nanotechnol.* **2**, 422–425 (2007).
12. J. E. Allen *et al.*, *Nat. Nanotechnol.* **3**, 168–173 (2008).
13. Y. Oshima *et al.*, *Phys. Rev. B* **81**, 035317 (2010).
14. H. Yoshida *et al.*, *Science* **335**, 317–319 (2012).
15. W. T. Yuan *et al.*, *Chem. Mater.* **29**, 3189–3194 (2017).
16. W. Yuan *et al.*, *Nano Lett.* **16**, 132–137 (2016).
17. M. Lazzeri, A. Selloni, *Phys. Rev. Lett.* **87**, 266105 (2001).
18. H. G. Yang *et al.*, *Nature* **453**, 638–641 (2008).
19. X. Han, Q. Kuang, M. Jin, Z. Xie, L. Zheng, *J. Am. Chem. Soc.* **131**, 3152–3153 (2009).
20. K. Fang *et al.*, *J. Phys. Chem. C* **123**, 21522–21527 (2019).
21. Y. Kuwauchi, H. Yoshida, T. Akita, M. Haruta, S. Takeda, *Angew. Chem. Int. Ed.* **51**, 7729–7733 (2012).
22. C. Arrouvel, M. Digne, M. Breysse, H. Toulhoat, P. Raybaud, *J. Catal.* **222**, 152–166 (2004).
23. C. Deiana, E. Fois, S. Coluccia, G. Martra, *J. Phys. Chem. C* **114**, 21531–21538 (2010).
24. J. Blomquist, L. E. Walle, P. Uvdal, A. Borg, A. Sandell, *J. Phys. Chem. C* **112**, 16616–16621 (2008).
25. I. Beinik *et al.*, *Phys. Rev. Lett.* **121**, 206003 (2018).
26. M. Duan *et al.*, *Angew. Chem. Int. Ed.* **57**, 6464–6469 (2018).
27. B. Zhu, Z. Xu, C. Wang, Y. Gao, *Nano Lett.* **16**, 2628–2632 (2016).
28. P. Panagiotopoulou, D. I. Kondarides, *J. Catal.* **225**, 327–336 (2004).
29. D. G. Rethwisch, J. A. Dumesic, *Appl. Catal.* **21**, 97–109 (1986).

ACKNOWLEDGMENTS

We gratefully acknowledge J. Fan (Department of Chemistry, Zhejiang University) for support and useful discussions.

Funding: We acknowledge the financial support of the National Natural Science Foundation of China (51390474, 91645103, 11574340, 21773287, 51801182, 11604357 51872260, and 11327901), the Zhejiang Provincial Natural Science Foundation (LD19B030001), the Ministry of Science and Technology of China (2016YFE0105700), and the Fundamental Research Funds for the Central Universities. B.Z. was supported by the Natural Science Foundation of Shanghai (16ZR1443200) and the Youth Innovation Promotion Association CAS. The computations were performed at the National Supercomputing Center in Guangzhou and Shanghai. W.Y. was supported by the China Postdoctoral Science Foundation (2018M642407 and 2019T120502). **Author contributions:** Y.W. initiated the work. Y.W., Y.G., J.B.W., and Z.Z. supervised the work. W.Y., Y.O., and K.F. synthesized the samples. W.Y. and T.W.H. conducted the ETEM experiments. Y.O. and H.Y. carried out the in situ FTIR experiments. B.Z. and X.Y.L. performed the calculations. All authors participated in the analysis and discussion. **Competing interests:** The authors declare no competing interests. **Data and materials availability:** All data needed to evaluate the conclusions in the paper are present in the paper, the supplementary materials, or the Cambridge Crystallographic Data Centre (deposition number: CSD 1970465-1970473).

SUPPLEMENTARY MATERIALS

science.sciencemag.org/content/367/6476/428/suppl/DC1
Materials and Methods
Supplementary Text
Figs. S1 to S14
References (*30*–*42*)
Movies S1 to S3
Appendix S1

2 June 2019; resubmitted 24 October 2019
Accepted 10 December 2019
10.1126/science.aay2474

Science

Visualizing H_2O molecules reacting at TiO_2 active sites with transmission electron microscopy

Wentao Yuan, Beien Zhu, Xiao-Yan Li, Thomas W. Hansen, Yang Ou, Ke Fang, Hangsheng Yang, Ze Zhang, Jakob B. Wagner, Yi Gao and Yong Wang

Science **367** (6476), 428-430.
DOI: 10.1126/science.aay2474

Imaging reactive surface water

Recent developments in transmission electron microscopy (TEM) have enabled imaging of single atoms, but adsorbed gas molecules have proven more challenging because of a lack of sufficient image contrast. Yuan *et al.* adsorbed water and carbon monoxide (CO) on a reconstructed nanocrystalline anatase titanium dioxide (TiO_2) surface that has protruding TiO_3 ridges every four unit cells, which provide regions of distinct contrast. Water adsorption on this surface during environmental TEM experiments led to the formation of twinned protrusions. These structures developed dynamic contrast as the water reacted with coexposed CO to form hydrogen and carbon dioxide.

Science, this issue p. 428